Temperature-dependent phase transitions in Pb(Zn1/3Nb2/3)0.93Ti0.07O3 crystal

Authors: R. R. Chien , V. Hugo Schmidt , Chi-Shun Tu , F. -T. Wang & L. C. Lim

R. R. Chien , V. Hugo Schmidt , Chi-Shun Tu , F. -T. Wang & L. C. Lim (2006) Temperature-Dependent Phase Transitions in Pb(Zn1/3Nb2/3)0.93Ti0.07O3 Crystal, Ferroelectrics, 339:1, 115-120, DOI: 10.1080/00150190600738089

Temperature-Dependent Phase Transitions in $Pb(Zn_{1/3}Nb_{2/3})_{0.93}Ti_{0.07}O_3$ Crystal

R. R. CHIEN,[1,*] V. HUGO SCHMIDT,[1] CHI-SHUN TU,[2] F.-T. WANG,[2] AND L. C. LIM[3]

[1]Department of Physics, Montana State University, Bozeman, MT 59717, U.S.A.
[2]Graduate Institute of Applied Science and Engineering, Fu Jen Univ., Taipei 242, Taiwan
[3]Department of Mechanical Engineering, National University of Singapore, Singapore 119260

The temperature dependent phase transitions in an unpoled (001)-cut $Pb(Zn_{1/3}Nb_{2/3})_{0.93}Ti_{0.07}O_3$ single crystal have been investigated by dielectric permittivity and polarizing microscopy. The crystal at room temperature has a dominant rhombohedral phase mixed with unknown domains. The unknown phase domains transform to coexistence of tetragonal/monoclinic symmetries near 350 K. As temperature increases, the tetragonal/monoclinic domains increase and reach saturation near 365 K. These phase transformations in the region of 350–365 K are responsible for the dielectric anomaly near 355 K. Most of monoclinic domains start to transform to the tetragonal domains near 422 K. The whole crystal becomes cubic phase at 432 K.

Keywords PZN-PT; phase transition; domains

Introduction

High-strain ferroelectric single crystals such as $Pb(Mg_{1/3}Nb_{2/3})_{1-x}Ti_xO_3$ (PMNTx) and $Pb(Zn_{1/3}Nb_{2/3})_{1-x}Ti_xO_3$ (PZNTx) have attracted much attention because they possess superior dielectric and electromechanical properties compared to lead zirconate titanate (PZT) ceramics and therefore have been used for designing high performance actuators and sensors [1–3]. Physical properties of PMNT and PZNT crystals strongly depend on titanium (Ti) content, temperature, electric (E)-field poling strength, crystallographic orientation, and history [4]. How the factors affect their physical properties still remains unclear and therefore should be investigated before they can be efficiently employed for applications. The structural and thermal phase stability are crucial for actuator and transducer designs. In this study, we investigate how temperature affects structures (phases) of PZNT7% single crystal. The crystal structure can in principle occur in the cubic (C), tetragonal (T), orthohombic (O), rhombohedral (R), monoclinic (M) and triclinic (*Tri*) phases.[5] All the phases except *Tri* phase have been observed in PMNT and PZNT crystals.

Paper originally presented at IMF-11, Iguassu Falls, Brazil, September 5–9, 2005; received for publication January 26, 2006.
*Corresponding author. E-mail: chien@physics.montana.edu

Experimental Procedure

The PZNT7% single crystal was grown using the modified flux method and was cut perpendicular to the [001] direction with the long edge orientations [100]/[010]. The sample dimensions are $4 \times 4 \times 0.09$ mm^3. For dielectric measurement, gold electrodes were deposited on sample surfaces by dc sputtering. A variable-frequency Wayne-Kerr Precision Analyzer PMA3260A with four-lead connections was used to measure capacitance and resistance, and to obtain real ε' and imaginary ε'' parts of dielectric permittivity. A Janis CCS-450 cold-head was used with a Lakeshore 340 temperature controller and the temperature ramping rate was 1.5 K/min. Before any measurement, the sample was annealed above T_m. Two processes were used in the dielectric measurements, i.e. "zero-field-heating" (ZFH) and "zero-field-cooling" (ZFC), in which the data were taken upon heating and cooling respectively without any E-field poling.

The domain structures were studied by using a Nikon E600POL polarizing microscope mounted with a Linkam THMS600 heating/cooling stage and the experimental configuration can be found in Ref. [6]. The [100] orientation of the sample edge was aligned with one of the crossed polarizer/analyzer (P/A): 0° axes for domain observation so that the extinction angles shown in all domain micrographs are measured from [100]. The sample was polished to the thickness of 90 μm. The domain observation was carried out upon heating by steps.

Results and Discussion

Figures 1(a) and (b) shows the temperature-dependent ε' and ε'' at several frequencies (0.5 kHz–1 MHz) obtained from ZFH and ZFC respectively. Frequency dispersion appears in both ε' and ε'' in a wide temperature region. However, the maximum temperatures are almost frequency-independent and can not be fitted by either the Vogel-Fulcher equation or Arrhenius law. The dielectric maximum temperatures T_m of ε' (ZFH) and ε' (ZFC) appear near 430 K where the tetragonal-cubic ferroelectric transition occurs. The insets of Fig. 1 show the reciprocal of ε' in which a typical first-order FE phase transition appears at $T_m \cong$ 430 K in both heating and cooling runs.

As shown in Fig. 2, both ε' and ε'' exhibit obviously wide thermal hystereses in the regions of ~200–360 K and ~400–430 K respectively, implying first-order transformations. In addition, ε' exhibits a weak shoulder upon cooling as indicated by a solid arrow in Fig. 2. It is important to note that dielectric absorptions ε'' (ZFH) and ε'' (ZFC) in the region of 200–360 K exhibit complex overlapping of at least two maxima. This maximum coupling implies a coexistence of different phases. Interestingly, a third dielectric anomaly associated with a dip was observed in both ε' and ε'' near 175 K upon cooling. However, it was not obviously seen upon heating, indicating different thermal activities between heating and cooling runs. This low-temperature anomaly possibly corresponds to a transformation below which all reorientation and coupling of clusters would cease, i.e. the "freezing" temperature is about 175 K.

In this study, polarizing microscopy reveals orientations of the polarizations and their corresponding phases by using relations of crystallographic symmetry and optical extinction. Optical extinction is the main principle used for determination of various phases (crystal symmetries). For interpreting domain structures observed by polarizing microscope, a review of principles of optical extinction for the (001)-cut crystal can be found in Refs. [7, 8]. As shown in Fig. 3(m), the inner square outlines the front face of the cube in the (001)-cut projection with all four sides folded out. Triangles, squares, and circles represent R, T, and O phase domains, respectively. The solid crosses in the symbols indicate the optical

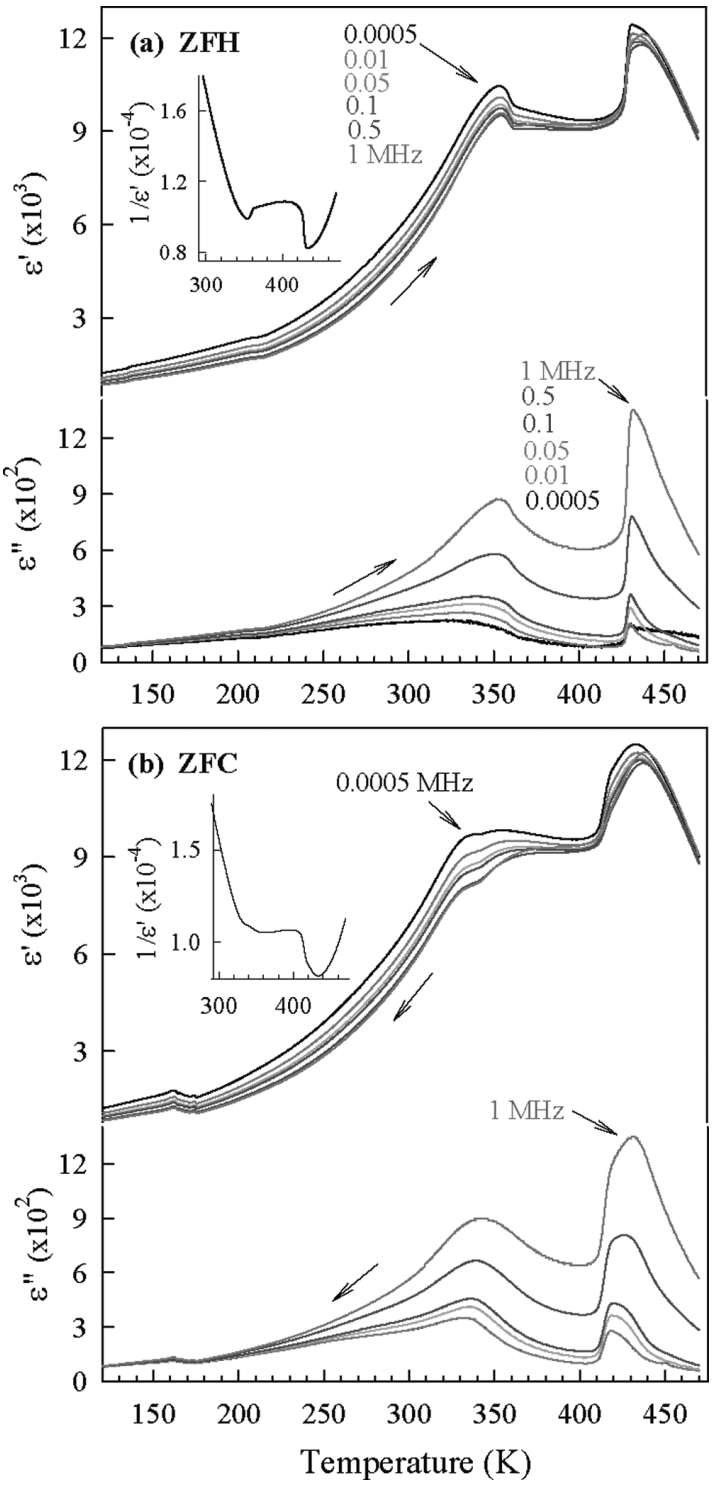

Figure 1. Dielectric permittivities (ε', ε'') of (a) ZFH and (b) ZFC at several frequencies. (See Color Plate VIII)

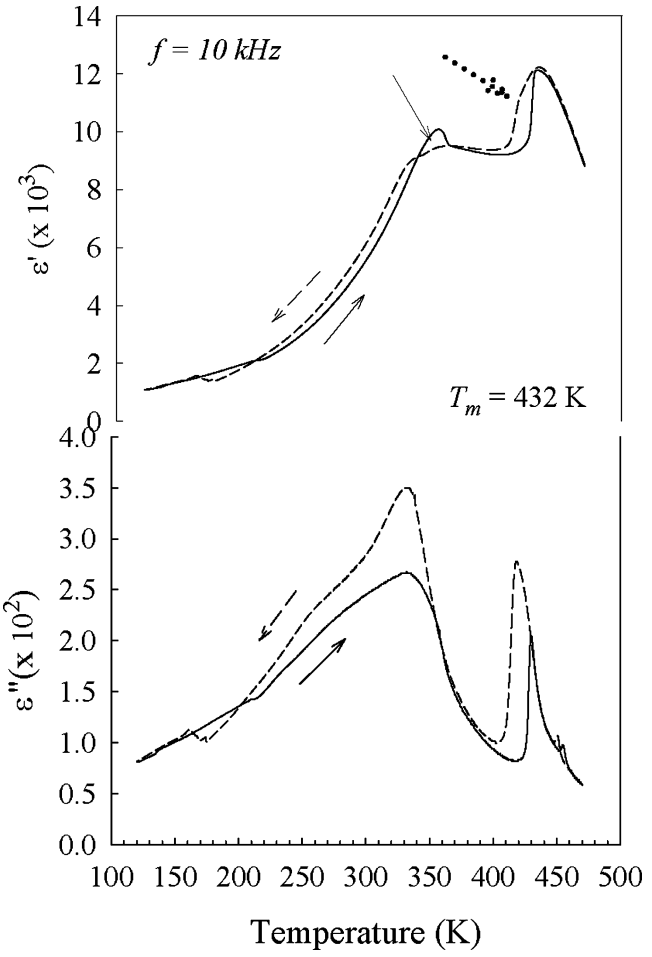

Figure 2. Real $\varepsilon'$and imaginary ε'' parts of dielectric permittivity measured at f =10 kHz.

electric field (polarization) axes **E** of the incident light for which extinction will occur for the corresponding domains. The square symbol shown in solid black at its center represents a T-phase domain whose **P** is parallel to the propagation direction **k** of the light, indicates that extinction occurs for all **E** directions because **E** is perpendicular to the optic axis for this optically uniaxial domain. Dashed, dash-dotted, and dotted lines represent M_A, M_B, and M_C phase domains, respectively. Measured from [100], the R and some O domains give extinction at 45°. The T and other O phase domains give extinction at 0° (or 90°). Any extinctions at angles other than 0° (=90°) and 45° must be from M or *tri* phase domains. Our large observed variation in extinction angle with temperature indicates M phase domains whose polarization P can vary with temperature through a large angle, whereas the direction of P is fixed for a given T, *O, or R* phase domain.

As shown in Fig. 3(a) and (b) at 295 K, a larger fraction of the unpoled sample exhibits extinction at P/A: 45°. But a small fraction (∼1/10), which does not exhibit extinction at any angle, is embedded in the domain matrix perhaps due to local strained regions caused by underlying M distortions with several different orientations. This indicates that the

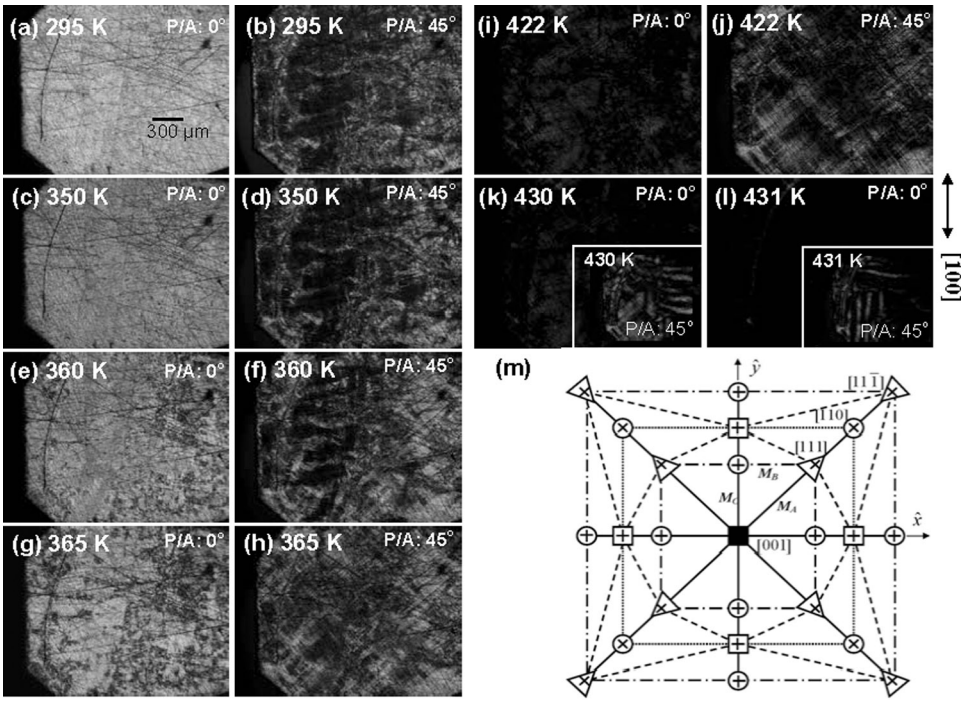

Figure 3. (a)–(l) Temperature-dependent domain micrographs observed at P/A: 0^o and P/A: 45°. (m) Relation between the optical extinction orientations corresponding to the polarizations for various phases and domains projected on the (001) plane.

unpoled sample has a dominant R phase mixed with some unknown phase (Y) domains, i.e. $R(Y)$. $R(Y)$ represents more R than Y phase volume. Note that O domains also have extinction at 45°. However, if O domains exist in the sample, extinction would likely also be seen at 0°, which was not found in this study as shown in Fig. 3(a). Near 350 K as shown in Fig. 3(c) and (d), the Y phase domains transform to coexistence of T and M symmetries *i.e. T/M*, where T is more than M phase domains. Thus, this Y phase likely has a unit cell with slight distortion from T or Msymmetries. The Y phase may be related to an unidentified phase (X) proposed in a PZNT 8% crystal.[9] Therefore, at 350 K the crystal has phase coexistence of $R(T/M)$. As temperature increases, the T/M domains increase at the expense of the Y domains [Fig. 3(e) and (f)] and reach saturation near 365 K [Fig. 3(g) and (h)]. In the meantime, the dominant R phase domains also start to transform to various M phase domains, which exhibit extinctions at P/A: 30–50°. As temperature increases a few more degrees, a long-range-order M phase was established between R and T phase domains. The M phase exhibits extinction at the P/A ranges of 25–30° and 50–60°. These phase transformations in the region of 350–365 K are responsible for the dielectric anomaly near 355 K. The long-range-order M phase domain expands extinction angle range from P/A: 25–30° and 50–60° to 0–25° and 60–85° as temperature increases to 422 K [Fig. 3(i) and (j)]. At 422 K, most of the M phase domains start to transform to T phase domains and some of the M phase domains persist to 430 K, where the cubic (C) phase begins to appear [Fig. 3(k)–(l) and the insets]. This is evidenced by an extra shoulder shown by the dotted arrow near 420 K upon cooling in ε' and the thermal hystersis

near 400–430 K as shown in Fig. 2. Some of the M phase domains transform to T phase before the whole crystal becomes C phase at 432 K. In brief, the phase transition sequence, $M/R/T \rightarrow M/T/R \rightarrow T/M$, takes place from 365 to 422 K. As temperature increases to 432 K, transformation of $T/M \rightarrow C$ takes place.

Conclusions

A thermal transition sequence, $R(Y) \rightarrow R(T/M) \rightarrow M/R/T \rightarrow M/T/R \rightarrow T/M \rightarrow C$, takes place in the (001)-cut PZNT7% crystal upon heating without poling (ZFH). $R(Y)$ indicates much more R than Y phase volume. $M/R/T$ represents a coexistence of M, R, and T phase domains with different portions obeying $M > R > T$. In this temperature dependent (without poling) transition, it was found that the M phase plays an important role of bridging between other phase regions while the phase transitions occur.

Acknowledgment

This work was supported by DoD EPSCoR Grant No. N00014-02-1-0657 and NSC Grant No. 93-2112-M-030-001.

References

1. J. Kumata, K. Uchino, and S. Nomura, Phase transitions in the $Pb(Zn_{1/3}Nb_{2/3})O_3$-$PbTiO_3$ system. *Ferroelectrics* **37**, 579 (1981).
2. T. R. Shrout, Z. P. Chang, N. Kim, and S. Markgraf, Dielectric behavior of single crystals near the (1-x)$Pb(Mg_{1/3}Nb_{2/3})O_3$-(x)$PbTiO_3$ morphotropic phase boundary. *Ferroelectrics Letters* **12**, 63 (1990).
3. S.-E. E. Park and W. Hackenberger, High performance single crystal piezoelectrics: applications and issues. *Curr. Opin. Solid State Mater. Sci.* **6**, 11 (2002).
4. B Noheda, Structure and high-piezoelectricity in lead oxide solid solution. *Curr. Opin. Solid State Mater. Sci.* **6**, 27–34 (2002).
5. D. Vanderbilt and M. H. Cohen, Monoclinic and triclinic phases in higher-order Devonshire theory. *Phys Rev B* **63**, 094108/1–9 (2001).
6. C.-S. Tu, V. H. Schmidt, I.-C. Shih, and R. Chien, Phase transformation via monoclinic phase in relaxor-based ferroelectric crystal $(PbMg_{1/3}Nb_{2/3}O_3)_{1-x}(PbTiO_3)_x$. *Phys. Rev. B(R)* **67**, 020102/1–4 (2003).
7. R. R. Chien, V. H. Schmidt, C.-S. Tu, L.-W. Hung, and H. Luo, Field-induced polarization rotation in (001)-cut $Pb(Mg_{1/3}Nb_{2/3})_{0.76}Ti_{0.24}O_3$. *Phys. Rev. B* **69**, 172101/1–4 (2004).
8. V. H. Schmidt, R. Chien, I.-C. Shih, and C.-S. Tu, Polarization rotation and monoclinic phase in relaxor ferroelectric PMN-PT crystal. *AIP Conference Proceedings* **677**, 160–167 (2003).
9. K. Ohwada, K. Hirota, P. W. Rehrig, Y. Fujii, and G. Shirane, Neutron diffraction study of field-cooling effects on the relaxor ferroelectric $Pb[(Zn_{1/3}Nb_{2/3})_{0.92}Ti_{0.08}]O_3$. *Phys. Rev. B* **67**, 094111/1–8 (2003).